

- NES, G. J. H. VAN & VOS, A. (1978). *Acta Cryst.* B34, 1947–1956.
- NES, G. J. H. VAN & VOS, A. (1979). *Acta Cryst.* To be published.
- PARK, Y. J., JEFFREY, G. A. & HAMILTON, W. C. (1971). *Acta Cryst.* B27, 2393–2401.
- RUYSINK, A. F. J. (1973). Thesis, Univ. of Groningen.
- RUYSINK, A. F. J. & VOS, A. (1974). *Acta Cryst.* B30, 1997–2002.
- STEWART, R. F. (1973). *J. Chem. Phys.* 58, 4430–4438.
- STEWART, R. F. (1974). VALRAY 1974 system. Department of Chemistry, Carnegie Mellon Univ., Pittsburgh, Pennsylvania, USA.
- STEWART, R. F. (1976). *Acta Cryst.* A32, 565–574.
- STEWART, R. F., BENTLEY, J. & GOODMAN, B. (1975). *J. Chem. Phys.* 63, 3786–3793.
- WAL, H. R. VAN DER (1979). Thesis, Univ. of Groningen.
- WAL, H. R. VAN DER & DE BOER, J. L. (1978). *Acta Cryst.* A34, S338.
- WAL, H. R. VAN DER, DE BOER, J. L. & VOS, A. (1979). *Acta Cryst.* A35, 685–688.
- WAL, H. R. VAN DER & VOS, A. (1979). *Acta Cryst.* B35, 1730–1732.
- WHITTAKER, E. & ROBINSON, G. (1949). *The Calculus of Observations*. London: Blackie.
- XRAY system (1976). Dutch version of the XRAY 76 system. Tech. Rep. TR-446. Computer Science Center, Univ. of Maryland, College Park, Maryland.

*Acta Cryst.* (1979). B35, 1804–1809

## Accurate Structure Determination of *trans*-2,5-Dimethyl-3-hexene-2,5-diol Hemihydrate, $C_8H_{16}O_2 \cdot \frac{1}{2}H_2O$ , at 86 K.

### II. Discussion of the Electron Density Distribution

BY H. R. VAN DER WAL AND AAFJE VOS

*Laboratorium voor Chemische Fysica, Rijksuniversiteit Groningen, Nijenborgh 16, 9747 AG Groningen, The Netherlands*

(Received 9 February 1979; accepted 19 March 1979)

#### Abstract

Experimental deformation densities for the title compound are compared with a smeared theoretical deformation density based on *ab initio* quantum-chemical calculations for a model compound (9,5,1/5,2 GTO basis set). Around the C–C bonds in the ethylene plane very good agreement with theory is obtained for the experimental  $D(HO, \mathbf{r})$  map. This map is based on high-order parameters of a conventional X-ray refinement, but with scale and overall thermal motion adjusted to full-angle data. Around the O atoms where  $D(HO, \mathbf{r})$  is not reliable, the theoretical map is compared with a multipole map not including monopole deformations and based on a multipole refinement with  $\zeta$  scattering factors. The multipole map clearly shows the influence of the hydrogen bonds on the deformation density.

#### 1. Introduction

In the previous paper (van der Wal & Vos, 1979; hereafter WV) the parameters obtained for the title compound by high-order X-ray refinement and multipole refinement have been discussed. In the present

paper the deformations in the electron density due to chemical bonding (bonding effects) are reported and compared with the bonding effects expected on the basis of quantum chemical calculations. The compound  $C_8H_{16}O_2 \cdot \frac{1}{2}H_2O$  will be referred to as II *trans A*.

#### 2. Experimental density distributions

##### Deformation density $D(HO, \mathbf{r})$

The observed deformation-density distribution is defined as

$$\begin{aligned}
 D(\mathbf{r}) &= Sc^{-1} \rho_o(\mathbf{r}) - \rho_c(\text{atoms}; \mathbf{r}) \\
 &= \sum_{\mathbf{H}} [Sc^{-1} F_o(\mathbf{H}) - F_c(\text{atoms}; \mathbf{H})] \\
 &\quad \times \exp(-2\pi i \mathbf{H} \cdot \mathbf{r}); \quad (1)
 \end{aligned}$$

$\rho_c(\text{atoms}; \mathbf{r})$  is based on spherically symmetric non-bonded atoms, Sc is the scale factor. The map has been calculated with the scale, positional and thermal parameters from the Sp(FA–HO) refinement discussed in WV. This implies that scale and overall thermal motion are adjusted to the full-angle data, whereas the

anisotropy of the thermal motion and the positional parameters correspond to reflections having  $\sin \theta/\lambda > 0.7 \text{ \AA}^{-1}$ . The map is based on reflections with  $\sin \theta/\lambda < 0.65 \text{ \AA}^{-1}$  and  $|F_o(\mathbf{H})| > 3\sigma[|F_o(\mathbf{H})|]$  and is denoted as  $D(\text{HO}, \mathbf{r})$  or HO map. The random error in  $D(\text{HO}, \mathbf{r})$  calculated according to Cruickshank (1949) is  $0.023 \text{ e \AA}^{-3}$ .

On the basis of the theoretical calculations on acetylene by Ruysink & Vos (1974*b*), we estimate that, due to the finite resolution,  $D(\text{HO}, \mathbf{r})$  is  $0.25 \text{ e \AA}^{-3}$  too high at the atomic positions, whereas the height of the maxima at the bond centers is hardly affected. Around the O atoms  $D(\text{HO}, \mathbf{r})$  is not reliable as the O atom is shifted too much towards the lone-pair region in the Sp(FA–HO) refinement.  $D(\text{HO}, \mathbf{r})$  will therefore not be used for the discussion of this region.

### Multipole maps

Multipole refinements with  $Z$  and  $P$  scattering factors have been discussed in WV. From the final difference maps after these refinements and the low  $R_w(I)$  values, 0.0082 and 0.0081 respectively, it follows that  $\rho_c(\text{multipole model}; \mathbf{r})$  gives a good filtered representation for  $K^{-1} \rho_o(\mathbf{r})$ . However, as was shown in WV,  $K$  is predominantly based on the high-order data and is thus not very reliable. Due to the correlation between  $K$ , the populations and the  $U_{ii}$  values, the latter quantities are also affected by systematic errors. Consequently  $\rho_c(\text{multipole model}; \mathbf{r})$  corresponds to an incorrectly scaled  $\rho_o(\mathbf{r})$  map, whereas  $\rho_c(\text{atoms}; \mathbf{r})$  contains incorrect  $U_{ii}$  thermal parameters. Especially at the atomic positions considerable errors are therefore expected for the multipole maps  $\rho_c(\text{multipole model}; \mathbf{r}) - \rho_c(\text{atoms}; \mathbf{r})$ . We have chosen to reduce these errors as much as possible by omitting the monopole deformations from the multipole maps. For the present case these maps are thus defined as

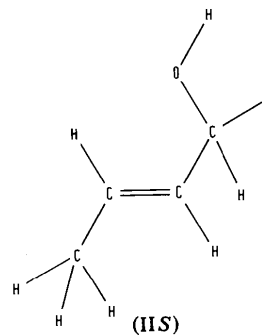
$$\begin{aligned} D_M(\mathbf{r}) &= \sum_{\mathbf{H}} [F_c(\text{dipole, quadrupole, octopole})] \\ &\times \exp(-2\pi i \mathbf{H} \cdot \mathbf{r}) \\ &= \sum_{\mathbf{H}} [F_c(\text{multipole model}; \mathbf{H}) \\ &- F_c(\text{monopoles}; \mathbf{H})] \exp(-2\pi i \mathbf{H} \cdot \mathbf{r}) \\ &= \rho_c(\text{multipole model}; \mathbf{r}) \\ &- \rho_c(\text{monopoles}; \mathbf{r}). \end{aligned}$$

For each multipole map a consistent set of parameters, including the radial functions, is used. The multipole map based on the model of the  $Z$  refinement will be denoted as  $D_M(Z, \mathbf{r})$  or  $Z$  map, and the map for the  $P$  refinement as  $D_M(P, \mathbf{r})$  or  $P$  map. For both maps account has been taken of reflections with  $\sin \theta/\lambda < 0.75 \text{ \AA}^{-1}$  and  $|F_o(\mathbf{H})| > 3\sigma[|F_o(\mathbf{H})|]$ .

Due to the omission of the monopole deformations, the  $D_M(\mathbf{r})$  densities do not represent the true bonding effect, especially at the atomic positions. Since for  $Z$  the calculated monopole populations are physically more realistic than for  $P$  we prefer the  $Z$  over the  $P$  maps. For  $Z$  the omission of the monopole deformations has the disadvantage, however, that changes in  $\zeta$  due to correlation with the monopoles are not balanced by changes in the monopole populations.

### 3. Theoretical deformation density distribution

As *ab initio* quantum-theoretical calculations for the crystal as a whole are not feasible, the computations have been done on individual molecules. Due to limitations in computing time and storage an even smaller model molecule IIS had to be chosen.



The atomic coordinates were taken equal to the  $Z$  refinement coordinates of the central part of II *trans A* (WV, Table 8). For C–H replacing C–C or C–O a reduction in length to  $1.08 \text{ \AA}$  was applied. The theoretical static deformation-density map is defined by

$$D_{\text{th}}(\text{static}; \mathbf{r}) = \rho_{\text{th}}(\text{static mol}; \mathbf{r}) - \rho_{\text{th}}(\text{atoms}; \mathbf{r})$$

with corresponding atoms at the same positions in the two maps. The static theoretical molecular density  $\rho_{\text{th}}(\text{static}; \mathbf{r})$  for IIS was obtained by the SCF–LCAO–MO method (Roothaan, 1951) with the program *BIGMOL* (van Duijnen & Thole, 1977). A GTO basis set (9,5,1 for both C and O and 5,2 for H) contracted to (4,2,1/4,2) was used for the calculation of the atomic and molecular wave functions.

The thermal parameters necessary for the smearing of the  $D_{\text{th}}(\text{static}; \mathbf{r})$  map with the program *BEDGOLV* (Ruysink & Vos, 1974*a*) were deduced from the II *trans A* U tensors of the  $Z$  refinement (WV, Table 8). The thermal motion of the central part of the molecule can reasonably be represented by the translations  $T_{11} = 0.00844$ ,  $T_{22} = 0.01162$ ,  $T_{33} = 0.01054 \text{ \AA}^2$  (referred to the crystal axes). The OH group and the H atoms of the CH<sub>2</sub> groups were given extra thermal vibrations (for  $U_{ii}$  coupled to  $T_{ii}$ ) represented by

$$\Delta U_{11} = 0.00247, \quad \Delta U_{22} = 0.00183,$$

$$\Delta U_{33} = 0.00177 \text{ \AA}^2 \text{ for O,}$$

$$\Delta U = 0.01810 \text{ \AA}^2 \text{ for H of OH,}$$

$$\Delta U = 0.01331 \text{ \AA}^2 \text{ for H of HC=CH,}$$

$$\Delta U = 0.01810 \text{ \AA}^2 \text{ for H of CH}_2.$$

The SCF-LCAO-MO *ab initio* calculations took about 14 c.p.u. hours on the Cyber 74-18, but the smearing with *BEDGOLV* is also very time consuming (for instance  $5\frac{1}{2}$  c.p.u. hours for the smearing of Fig. 3d).

#### 4. Experimental deformation densities for C—C

In Table 1 average values are listed for the heights of the maxima on the C—C bonds. The r.m.s. deviation for the average values is given by

$$d = \left\{ \sum_i [D(b_i) - \bar{D}(b)]^2 / [n_b(n_b - 1)] \right\}^{1/2},$$

with  $D(b_i)$  the value for bond  $b_i$  of type  $b$ , and  $n_b$  the number of bonds  $b$ . For the four  $C(sp^3)$ — $C(sp^3)$  bonds the r.m.s. value for  $Z$  is higher than for  $P$  and  $HO$ . We have ascribed this relatively large r.m.s. value for the  $Z$  map to the fact that in this map differences in  $\zeta$  are not balanced by monopole variations. As expected, for all three maps the bond maxima increase in the order:  $C=C > C(sp^2)$ — $C(sp^3) > C(sp^3)$ — $C(sp^3)$ . For the C—C single bonds the  $D(HO, r)$  values are higher than

Table 1. Height of the maxima at C—C bond centers

Average values are given with r.m.s. deviations in parentheses.

Bond type	$D_M(Z, r)$	$D_M(P, r)$	$D(HO, r)$
C=C	0.570	0.590	0.587
$C(sp^2)$ — $C(sp^3)$	0.412 (13)	0.450 (2)	0.494 (20)
$C(sp^3)$ — $C(sp^3)$	0.381 (16)	0.385 (13)	0.431 (7)

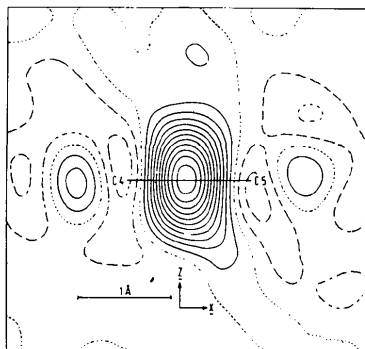


Fig. 1. Section of the  $D(HO; r)$  map perpendicular to the ethylene plane and through  $C=C$ . Contours in this and following figures are at intervals of  $0.05 \text{ e \AA}^{-3}$ . Full lines are positive, dotted lines zero and dashed lines negative contours.

$D_M(Z, r)$  and  $D_M(P, r)$ . That this is not the case for the  $C=C$  double bond has been ascribed to the fact that for  $HO$   $C(4)$  and  $C(5)$  of the double bond are slightly closer to the bond center than for  $Z$  or  $P$  (WV, § 7). Fig. 1 shows that this small shift obscures the quadrupolar-type deformation generally observed around the ethylene  $C$  atoms (compare Fig. 3e–f). Therefore for the discussion of this quadrupolar-type deformation the  $HO$  map cannot be used.

In Fig. 2 spherical averages of the densities in the sections perpendicular to the C—C double and single bonds and passing through the respective bond centers are given for  $Z$  and  $HO$ . The numbers in the figure are the asphericity parameters defined by

$$As = r(D = \frac{1}{2}D_{\max}, r_1) / r(D = \frac{1}{2}D_{\max}, r_2),$$

where  $r_1$  and  $r_2$  are the directions with the largest and smallest variation in  $D(r)$  respectively. For the single bonds the  $As$  parameters do not deviate too much from 1. Average values are 0.95 for  $HO$  and 0.89 for  $Z$ . As expected, for the non-cylindrical density around the double bond the  $As$  parameter is smaller, the average value for  $HO$  and  $Z$  being 0.74.

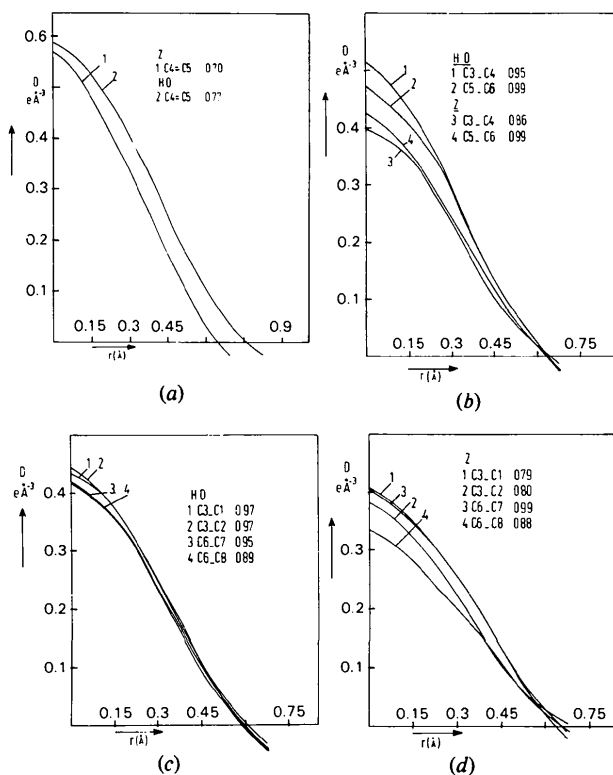


Fig. 2. Spherically averaged deformation density for  $HO$  and  $Z$  in the plane perpendicular to C—C and through the bond center, as a function of the distance  $r$  ( $\text{\AA}$ ) from the bond center. The numbers in the figures are the asphericity parameters defined in the text.  $C(4)$  and  $C(5)$  are the atoms of the double bond;  $C(3)$ — $C(4)$  and  $C(5)$ — $C(6)$  are  $C(sp^2)$ — $C(sp^3)$  bonds, and the remaining C—C bonds are  $C(sp^3)$ — $C(sp^3)$  bonds.

### 5. Experimental and theoretical densities around C—C and C—H

In Fig. 3(a)–(f) sections of the experimental and theoretical deformation densities are given. Fig. 3(a)–(c) shows the experimental  $P$ ,  $Z$  and HO maps for the plane  $C(3)C(4)C(5)$ . Qualitatively the three maps are the same; some quantitative differences have been discussed in the previous sections. For the theoretical density (Fig. 3d) it may be noted that the bonding maximum at  $C(5)–C(6)$ , lying on the O atom side of the molecule, is higher than at  $C(3)–C(4)$ . This shows that the bonding maxima do not depend only on the type of bond, but also on its surroundings. Moreover,  $C(5)$  lies at a higher level than  $C(4)$ , indicating that

charge has moved in the direction of the more electro-negative O atom. For comparison with the experimental II *trans A* maps the  $=C(5)–C(6)(H_2)–OH$  part of IIS will be used. In Fig. 3(c) and (d) the HO map is compared with the smeared theoretical density in the plane  $C(3)C(4)C(5)$ . In Fig. 3(e) and (f), a comparison is made between the experimental  $Z$  and the theoretical map for the section perpendicular to  $C(3)C(4)C(5)$  and through  $C=C$ . In Table 2 theoretical and experimental densities for the C—C bond region are listed.

Fig. 3(c) and (d) shows that the theoretical density around C—H is larger than the experimental. This is due to the fact that in the theoretical deformation map diffuse free H atoms are subtracted rather than the contracted H atoms used for the experimental map.

Table 2 shows that, after correction of the experimental densities for finite resolution, the agreement with theory is surprisingly good. Also the general trends in the relevant parts of Fig. 3(c) and (d) are seen to be similar if account is taken of the finite resolution of the experimental map. This indicates that indeed the Sp(FA—HO) refinement has given the correct scale factor and overall thermal motion. In view of the fact that the theoretical density is calculated for a model molecule, whereas the experimental one is based on parameters which may be slightly in error, it cannot be excluded that the two maps show small errors with a comparable trend. The good agreement seems to show, however, that in the C—C region the density is not affected much by the intermolecular interactions (hydrogen bonding) in the crystal. With due account of the fact that, because of the omission of the monopole deformation,  $D(Z, r)$  is too flat at the C positions, the deformation densities of Fig. 3(e) and (f) are also similar. The theoretical bonding maximum is somewhat more extended in the  $Z$  (or  $\pi$ ) direction than the experimental one. The relatively low values observed in Fig. 3(e) at  $C(4)$  for the minima above and below  $C(4)–C(5)$  are due to the relatively low  $\zeta$  value for  $C(4)$ , in comparison with  $C(5)$  (WV, Table 8).

In the following paper (de Boer & Vos, 1979) the deformation densities for the C—C bonds will be compared with the densities in other molecules with single, double or triple bonds.

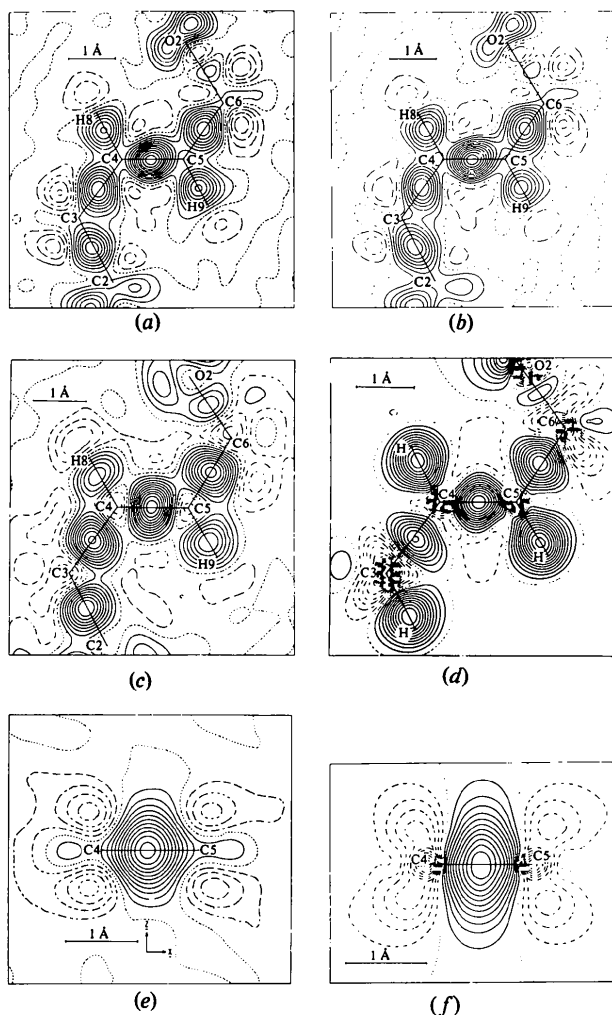


Fig. 3. Sections of the experimental and theoretical deformation-density distributions. (a–d) In the  $C(3)C(4)C(5)$  plane, (e) and (f) in the plane through  $C=C$  and perpendicular to  $C(3)C(4)C(5)$ . (a)  $D_M(P, r)$ , (b)  $D_M(Z, r)$ , (c)  $D(HO, r)$ , (d)  $D_{th}(r)$ , (e)  $D_M(Z, r)$ , (f)  $D_{th}(r)$ .

Table 2.  $D(r)$  values ( $e \text{ \AA}^{-3}$ ) at bond centers and at atomic positions for  $D(HO, r)$  and  $D_{th}(r)$

$D(\text{corr}; HO, r) = D(HO, r)$  for bonding maxima, and  $D(\text{corr}; HO, r) = D(HO, r) - 0.25$  at atomic positions.

	$D(HO, r)$	$D(\text{corr}; HO, r)$	$D_{th}(r)$
$C(4)–C(5)$	0.59	0.59	0.59
$C(5)–C(6)$	0.48	0.48	0.49
$C(5)$	–0.16	–0.41	–0.44
$C(6)$	–0.27	–0.52	–0.53

### Influence of hydrogen bonding on the density around oxygen

Before the influence of the hydrogen bonds is discussed, the density in the C—O bonds and the average density in the lone-pair region will be considered. For C—O we see in the theoretical density of Fig. 3(d) a moderate increase from a negative value of  $-0.53 \text{ e } \text{Å}^{-3}$  at C(6) to a maximum value of  $0.15 \text{ e } \text{Å}^{-3}$ , followed by a sharp decrease. This decrease does not show up in the experimental maps of Fig. 3(a) and (b), because of their finite resolution. As a consequence of this flattening the experimental C—O bond maxima are lower than the theoretical value. Fig. 4(c) shows the smeared theoretical density for the plane perpendicular to C—O—H and bisecting the C—O—H angle. Fig. 4(a) and (b) gives corresponding sections of the experimental  $D_M(Z, r)$  map for the two independent O atoms. In both the theoretical and experimental maps the O atom lies at a slope. However, in the experimental maps the slope is flattened due to their finite resolution. On average the height and shape of the experimental lone-pair regions show reasonable agreement with theory.

### Hydrogen bonding

The essential difference between the theoretical and experimental situation is that the theoretical calculations have been made for an isolated IIS molecule,

whereas in reality the molecules are placed in a crystal field. In the present case the intermolecular interaction is reasonably strong, because of the presence of hydrogen bonds (WV, Fig. 1). The experimental maps clearly show the influence of the crystal field on the electron density distribution. Whereas the theoretical map is approximately symmetric about the bisector  $b$ , the experimental map shows a concentration of O atom lone-pair electrons around the hydrogen bond. The chance that this phenomenon is not real is negligibly small, as the effect is clearly visible for both independent O atoms. A similar effect, but to a smaller extent as only  $D(HO, r)$  maps were used, has been detected by Helmholdt & Vos (1977) in the analogous compound with a triple C≡C bond.

An extensive review of the influence of hydrogen bonding on electron density distributions has been given by Olovsson (1978). Both experimental and theoretical deformation maps are discussed and some preliminary conclusions (because of possible errors in the experimental maps and the limited basis sets for the theoretical calculations) are drawn. The theoretical calculations, for instance on the  $H_2O$  dimer (Yamabe & Morokuma, 1975), show that the change in density distribution due to hydrogen bonding can largely be explained by polarization. Changes due to other effects, such as exchange and charge transfer, almost cancel each other out. Therefore for the water dimer, Olovsson's (1978) preliminary conclusion is that

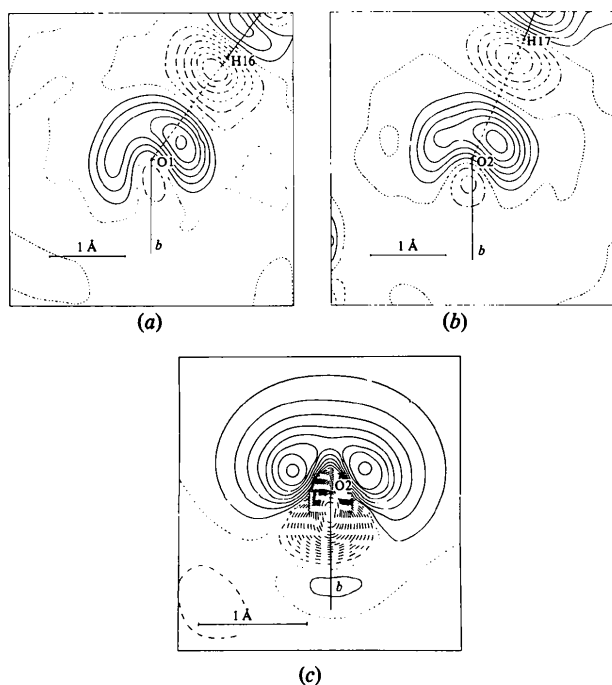


Fig. 4. Deformation densities for the O atom lone-pair regions. The sections are perpendicular to the respective C—O—H planes and bisect the C—O—H angles.  $b$  = bisector of C—O—H. Hydrogen bonds are indicated by dashed lines. (a)  $D_M(Z, r)$  for O(1), (b)  $D_M(Z, r)$  for O(2), (c)  $D_{th}(r)$ .

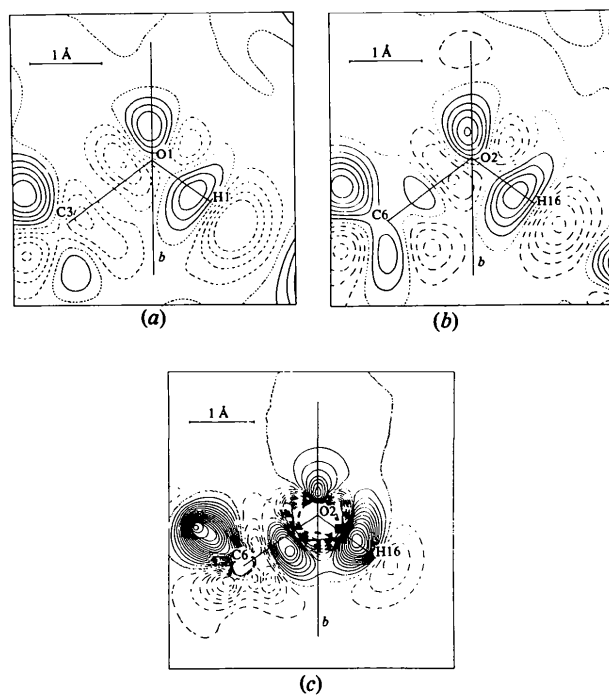


Fig. 5. Deformation densities in the C—O—H plane. (a)  $D_M(Z, r)$  for O(1), (b)  $D_M(Z, r)$  for O(2), (c)  $D_{th}(static; r)$ .

hydrogen bonding increases the polarity in the parts which are directly participating in the hydrogen bond. The present study shows that this conclusion also holds for the proton-accepting O atom lone-pair regions in II *trans A*.

It should be borne in mind that the O atoms in II *trans A* are not only H acceptors, but also H donors (WV, Fig. 1). According to Olovsson's conclusion this should increase the O atom lone-pair density at the extension of the H—O bond. Whether or not this is correct for II *trans A* can be studied for sections through the C—O—H plane (Fig. 5*a-c*). We see that for both O atoms the experimental  $D_M(Z, r)$  sections indeed show a slight inclination of the O atom lone-pair lobe towards the extension of the H—O bond. The theoretical (static, because of the large computing time needed to smear the density) map for the isolated IIS molecule, on the other hand, shows (Fig. 5*c*) a slight inclination of the lobe in the opposite direction, thus towards the (positively charged) H atom, as might be expected.

Further experimental and theoretical work on the influence of hydrogen bonding on density distributions is evidently required. Experimentally the positions of H and O should be determined accurately by neutron diffraction. On the theoretical side calculations with more extended basis sets and making reasonable allowance for the crystal field are necessary.

*Acta Cryst.* (1979). B35, 1809–1812

## Electron Density Distributions on C—C Single, Double and Triple Bonds. Pitfalls and Prospects of the Analysis of Accurate X-ray Diffraction Data

BY J. L. DE BOER AND AAFJE VOS

*Laboratorium voor Chemische Fysica, Rijksuniversiteit Groningen, Nijenborgh 16, 9747 AG Groningen, The Netherlands*

(Received 9 February 1979; accepted 19 March 1979)

### Abstract

Results obtained so far at Groningen for electron densities of compounds having single, double and triple C—C bonds are compared with each other and with densities from *ab initio* theoretical calculations. Suggestions for the improvement of further electron density studies and for the determination of physical properties from diffraction data are made.

### Experimental and theoretical data

Now that accurate density distributions have been obtained for different compounds with C—C single,

We thank Drs Th. Thole and Dr H. van Piggelen for their help with the quantum-theoretical calculations, and Dr J. L. de Boer for reading the manuscript. Part of the work has been supported by the Foundation for Fundamental Research of Matter with X-rays and Electron Rays (FOMRE) with financial aid from the Netherlands Organization for the Advancement of Pure Research (ZWO). The computations were carried out at the computer center of the University of Groningen.

### References

- BOER, J. L. DE & VOS, A. (1979). *Acta Cryst.* B35, 1809–1812.  
 CRUICKSHANK, D. W. J. (1949). *Acta Cryst.* 2, 65–82.  
 DULINEN, P. TH. VAN & THOLE, B. T. (1977). *BIGMOL*. Laboratory of Chemical Physics, Univ. of Groningen.  
 HELMHOLDT, R. B. & VOS, A. (1977). *Acta Cryst.* A33, 456–465.  
 OLOVSSON, I. (1978). *Crystal Forces and Hydrogen Bonding. Effect on Charge Density*. Laboratoire de Cristallographie, CNRS, Grenoble.  
 ROOTHAAN, C. C. J. (1951). *Rev. Mod. Phys.* 23, 69–89.  
 RUYSINK, A. F. J. & VOS, A. (1974*a*). *Acta Cryst.* A30, 497–502.  
 RUYSINK, A. F. J. & VOS, A. (1974*b*). *Acta Cryst.* A30, 503–506.  
 WAL, H. R. VAN DER & VOS, A. (1979). *Acta Cryst.* B35, 1793–1804.  
 YAMABE, S. & MOROKUMA, K. (1975). *J. Am. Chem. Soc.* 97, 4458–4465.

double and triple bonds, an evaluation of the results should be attempted. Accurate X-ray diffraction intensities have been measured for ethylene (van Nes & Vos, 1979), acetylene (van Nes & van Bolhuis, 1979) and for the compounds II.  $\frac{1}{2}$ H<sub>2</sub>O (van der Wal, 1979; van der Wal & Vos, 1979*a,b*) and III (Helmholdt & Vos, 1977).

